ELSEVIER

Chemical Engineering Journal 84 (2001) 239–245

Chemical Engineering Journal

www.elsevier.com/locate/cej

Investigation of the interaction of velocity and concentration fields by coupling LDV to conductivity probe in a continuous stirred tank reactor (CSTR)

S. Benayad [a], A. Salem [b], J. Legrand [c,*]

[a] *Institut Algérien du Pétrole, Boumerdès 35000, Algeria*

[b] *Laboratoire de Mécanique des Fluides, Institut de Physique, USTHB, Bab Ezzouar, Algeria*

[c] *Laboratoire de Génie des Procédés-UPRES EA 1152, CRTT-IUT-BP406-44602, Saint Nazaire, France*

Accepted 15 October 2000

Abstract

Velocity and concentration fields interaction has been experimentally investigated by mixing pure and salty water in a continuous stirred tank reactor. This has been achieved by coupling LDV and conductivity system which led to velocity–concentration correlations and to turbulent diffusivity. The axial velocity–concentration correlation coefficient does not exceed 5% in the turbine plan and below it. The knowledge of both concentration gradient and turbulent flux allowed the determination of turbulent diffusivity. The assumption of turbulence isotropy is discussed. Except in the immediate proximity of the stirrer, the probability density function of either velocities and concentration does not deviate significantly from Gaussian distribution indicating, in agreement with literature, local isotropy conditions particularly in the upper part of the tank with respect to the stirrer. The obtained results will contribute to refined mixing models while improving scale up procedures.

Keywords: Mixing; Reactor; LDV; Conductivity; Turbulence

1. Introduction

The optimisation of chemical reactor performance may be obtained through a deeper knowledge of chemical kinetics and of dynamic conditions which control the mixing of the reactant species. Indeed, small concentration fluctuations may have important effects on the final product quality which strongly depends on hydrodynamics and turbulence generated by the agitation allowing the intimate contact between the reactants. Thus, any attempt of reactor design and scale-up optimization requires a good understanding of the micromixing process as well as an acute analysis of these phenomena.

In the case of agitated vessels, two experimental mixing approaches can be considered. The first type is used by chemical engineers by using the concept of residence time distribution (RTD), mixing precocity and segregation intensity. The second type is based on fluid dynamics methods by characterizing the micromixing on the basis of turbulence theory concepts. In fact, the two ways are complementary.

The present paper deals with a configuration close to the standard reactor [1,2]. The velocity field has been extensively studied [3–14] as well as some turbulence characteristic parameters such as microscales [3,4,7,9,10,15–18] or integral scales [5,7,9,10,12,17,19,20]. Nagata [15] has found that the dissipation scale is maximum near the impeller and minimum in the reactor "eye". These results were further confirmed by Barthole et al. [7] and Nishikawa et al. [16]. Near the impeller area, Taylor microscale is in the range $0.016–0.09w$ and $0.003–0.039w$ far from the stirrer zone [5,7,9,10,16]; Stahl Wermesson and Tragarth [18] have found values three times greater. For Costes and Couderc [17], the integral scale Λ_i relative to any velocity component is independent of the stirrer rotational speed N but proportional to the tank diameter D. On the other hand, the scales Λ_i relative to the three velocity components are of the same order of magnitude comprised between $0.1–1.0w < \Lambda_i < 0.3–3.0w$ [5,9,10,17,19,20] (w being the turbine blade height). The highest values are reported by Costes and Couderc [17].

The parameters related to the local nature of turbulence were the object of relatively few works. Most authors assume isotropic turbulence when determining the turbulence

* Corresponding author.
E-mail address: jack.legrand@lgp.univ-nantes.fr (J. Legrand).

1385-8947/01/$ – see front matter
PII: S1385-8947(00)00280-1

Nomenclature

b	baffle width (cm)
c	concentration fluctuation (mol m^{-3})
$\overline{c v_i}$	turbulent flux (mol m^{-2} s^{-1})
$C(t)$	instantaneous concentration (mol m^{-3})
CTA	constant temperature anemometry
D_i	stirrer diameter (m)
D_m	molecular diffusion coefficient (m^2 s^{-1})
D_t	turbulent diffusion coefficient (m^2 s^{-1})
$E(t)$	residence time distribution (RTD) (s^{-1})
F	flatness factor (dimensionless)
g	diameter of the turbine disc (cm)
h	blade width (cm)
H_i	distance between tank bottom and turbine (cm)
k	velocity or concentration fluctuation
N	stirrer rotational speed (s^{-1})
P	dissipative power per unit of mass (m^2 s^{-3})
q	turbulent kinetic energy (m^2 s^{-2})
Q	flow rate (cm^3 s^{-1})
r	radial coordinate (m)
r^+	dimensionless radial coordinate, $r^+ = 2r/D_i$ (dimensionless)
Re	Reynolds number (dimensionless)
R_{cvi}	velocity–concentration correlation coefficient (dimensionless)
R_{cvz}	axial velocity–concentration correlation coefficient (dimensionless)
R_E	Euler correlation
S	skewness factor (dimensionless)
Sc	Schmidt number (dimensionless)
S_{con}	skewness factor relative to the concentration (dimensionless)
t	time (s)
T	tank diameter (cm)
U	tip speed, $U = \pi N D_i$ (m s^{-1})
$\bar{U}$	local mean velocity (m s^{-1})
v_i	velocity fluctuation in a general case (m s^{-1})
v_o	tangential velocity
v_r	radial velocity
v_z	axial velocity
V_c	convection velocity (m s^{-1})
V_{ol}	reactor volume (m^3)
V_i	velocity in a general case (m s^{-1})
w	blade height (cm)
Z	axial coordinate (m)
Z^+	dimensionless axial coordinate, $Z^+ = 2Z/w$ (dimensionless)

Greek symbols

ε	kinetic energy dissipation rate (m^2 s^{-3})
γ	intermittency factor (dimensionless)
Λ_i	integral scale (m)
ν	kinematic viscosity (m^2 s^{-1})
θ	temperature (°C)
τ	residence time or time delay (s)

Superscripts

–	average
+	dimensionless parameter

Subscripts

con	concentration
i	integral (scales)
inj	injected (e.g., C_{inj}: concentration of injected solution)
iv_o	i for integral (scale) and v_o for tangential velocity component
k	relative to fluctuation k
o	tangential
r	radial
z	axial

kinetic energy dissipation rate ε. Nevertheless, it is to be mentioned that near the impeller velocity, fluctuations are negatively skewed and hence significantly different from normal distribution [4,5]. In a general manner, there is a deviation from isotropy only in the immediate proximity of the impeller; far from the turbine, the turbulence may be considered as isotropic [9,13,16,20,21]. Rutherford et al. [22] did the same observation in the case of a tank stirred by two Rushton turbines. The convection velocity V_c has been measured using optical means in a standard tank by Michelet et al. [20] and by Stahl Wermesson and Tragarth [14] using constant temperature anemometry (CTA) technique in a vessel stirred by two Rushton turbines. The former [20] reported that this parameter decreases along the tank radius but remains greater than the local mean velocity and the latter [14] have observed that V_c is of the order of 1.6 times the local mean velocity.

The results dealing with turbulent diffusion or velocity–concentration correlations are scarce. Nagata [15] has described the dispersion coefficient distribution obtained by measuring the extent of the plume following a dye injection. In an axisymmetric jet flow, this parameter was studied using an LDV–laser-induced fluorescence coupling procedure by Lemoine et al. [23,24]. On the other hand, Benayad et al. [21] reported some results on the velocity–concentration correlation coefficients and showed that these coefficients are positive and do not exceed 5% in the area immediately in front and above the impeller.

The concentration field has been investigated either by electrochemical [3,4,7,12,25] or by optical methods [26]. Most authors have observed that in the case of perfectly macromixed reactor, the mean local concentration may be considered as constant within an error of 5% [3,25]. The perfect macromixing is characterized by an exponentially

decreasing RTD ($E(t) = 1/\tau \exp(-t/\tau)$) with $\tau = V_{ol}/Q$ is the ratio of the reactor volume V_{ol} to the feeding flow rate Q. The segregation index $(\overline{c^2})^{1/2}/\bar{C}$ has been, also, intensively studied [3,4,7,12,25,27]. It reaches $3–7 \times 10^{-3}$ [25,27] in a small reactor and can attain values as low as 10^{-4} [7] in a larger reactor.

When considering numerical predictions and mixing models, many parameters must be investigated [9,28] and many assumptions need to be strengthened by experimental data prior to any attempt of full-scale application [29]. Nevertheless, turbulence parameter measurements in the vessel complex flow are by no means easy and many related questions are not yet answered. For example, data on velocity–concentration correlation or turbulent diffusion coefficient are scarce although Benayad et al. [21] and Nagata [15] have reported some indications. The velocity–concentration correlation coefficient and the turbulent diffusion coefficient are, respectively, of the order of 5% [21] and $10\,cm^2\,s^{-1}$ [15]. One of the main reasons is that contrarily to mean velocities and concentration measurements which are relatively easy, the $\overline{c v_i}$ term expressing the interaction between velocity and concentration fields necessitates sophisticated measurements. Indeed, their calculation requires local and simultaneous acquisition of velocity and concentration measurements. For this goal, an laser Doppler velocimetry (LDV) system is coupled to a microconductivity probe in a 6.3 l, fully baffled, continuously fed standard reactor agitated by a six-flat blade Rushton turbine. Conductivity is easy to run and is commonly used for macro-micromixing measurements, including the industrial scale. The main objective of this contribution is to obtain more information on the turbulence characteristics, to determine the axial velocity–concentration correlation in the stirrer plan and below it prior to discussing the turbulent diffusion coefficient. Thus, in four axial tank plans, we have analyzed:

- the skewness and flatness factors of the three velocity components,
- the concentration and the tangential velocity integral scales,
- the axial velocity–concentration correlation coefficient, and
- the turbulent diffusion coefficient.

Many authors have observed and analyzed the periodic phenomenon induced by the turbine blades' rotation [5,6,9,10,20]. All authors emphasize its influence in the area of the impeller and conclude to the predomination of random turbulence for $r^+ > 1.4–1.8$ [12,20]. Lee and Yianneskis [9] reported that the magnitude of the peak relative to the period phenomenon in the velocity spectra at $r^+ = 1.32$ is about 20% of the one observed at $r^+ = 1.02$ and this peak disappears at $r^+ = 1.5$. Then, the velocity fluctuations are considered as purely turbulent in the experimental conditions investigated in this work.

2. Measurement techniques and calculations procedure

2.1. Measurement techniques

The instantaneous local concentration is measured by a microconductimetry technique described by Benayad [3] and Brodberger [25]. The conductivity microprobe is made of a platinum 30 μm diameter wire fitted in a 0.8 mm diameter and 40 mm long glass tube. The platinum wire is maintained by means of a seal as described in [3]. The microprobe active area is the wire cross-section which is electrochemically platinated before each run. The conductivity system is a squarewave one with a relatively high frequency response (200 Hz).

The instantaneous velocities are measured by LDV following the differential fringes procedure. The LDV system is a one-component type provided with a Bragg cell enabling measurement in reverse flow conditions. Due to optical constraints, the radial velocity component measurements were limited to the radius range $r^+ = 6r/D < 1.40$ (D is the tank diameter). Indeed, the tank cylindrical reactor has a circular cross-section; laser beams are only affected by refraction on the diopter air-PMMA when directed to the tank center. The beams are totally reflected when the bisector of the angle they form is parallel to a line passing through the center but shifted by a quantity $r^+ > 1.40$ with respect to this line. This case excludes all radial velocity measurement. Fortunately, in presence of refraction ($r^+ < 1.40$), the measurement is possible but the actual position of the laser beams intersection, i.e. the LDV measurement volume location, has to be recalculated.

In view to achieve the coupling between the velocity and concentration measurement devices without any hydrodynamic disturbance, particular attention was paid to fulfil the conditions prescribed by Benayad [3] when positioning the microprobe with respect to the laser beams intersection. The concentration and velocity fluctuations $c(t) = C(t) - \bar{C}$, and $v_i(t) = V_i(t) - \overline{V_i}$ are converted into analogical signals respectively through the conductivity system and the LDV frequency tracker. The signals are, then, sampled with respect to Shannon criterion prior to their numerical conversion; energy spectra and probability density functions (PDF) are then calculated.

2.2. Calculation procedure

The integral scale Λ_{ik} relative to a fluctuation $k(t)$ is determined by the Eulerian time correlation which gives

$$\Lambda_{ik} = \bar{U} \int_0^\infty R_E \, dt \tag{1}$$

where $\bar{U}$ is the local mean velocity and

$$R_E(\tau) = \frac{\overline{k(t)^* k(t-\tau)}}{\overline{k^2}} \tag{2}$$

Table 1
Stirred tank reactor experimental conditions

Reactor volume	$V_{ol} = 0.0063\,m^3$
Stirrer diameter	$D_i = 66.6\,mm$
Rotational speed	$N = 6.8\,s^{-1}$
Flow rate in the reactor	$Q = 150\,cm^3s^{-1}$
Injected KCl solution flow rate	$Q_{inj} = 2.12\,cm^3s^{-1}$
Injected KCl solution concentration	$C_{inj} = 160–320\,mol\,m^{-3}$
Temperature	$\theta = 25 \pm 0.5°C$ [30]
Molecular difussion coefficient	$D_m = 1.917 \times 10^{-5}\,cm^2\,s^{-1}$ [30]
Schmidt number	$Sc = v/D_m = 467$
Turbine Reynolds number	$Re = UD_i/v = 106\,000$
Dissipated power per unit of mass	$P = 5N^3D_i^5/V_{ol} = 0.33\,m^2\,s^{-3}$ (or W/kg)

The velocity–concentration correlation coefficients are defined by

$$R_{cvi} = \frac{\overline{cv_i}}{\sqrt{\overline{v_i^2}}\sqrt{\overline{c^2}}} \quad (3)$$

and calculated from the cross-correlation curves obtained by use of the reverse FFT of the interspectra. The knowledge of the flux $\overline{c_{v_r}}$ as well as concentration gradient and the use of Boussinesq hypothesis allows to estimate the radial turbulent diffusivity D_t

$$\overline{c_{v_r}} = -D_t \frac{\partial \bar{C}}{\partial r} \quad (4)$$

3. Experimental apparatus

A standard tank built in a cube of PMMA is continuously fed by a constant temperature premixed stream of pure water and KCl solution through a hole of 30 mm diameter drilled in the plan base. Stirring is achieved by a six-flat blade Rushton turbine. A passive contaminant, a KCl solution, is injected axially in the pipe supplying the tank. The discharge occurs by overflow.

The experimental conditions are illustrated in Table 1; tank characteristics presented in Fig. 1, and the dimensionless coordinates used in Fig. 2. It is to be noticed that the

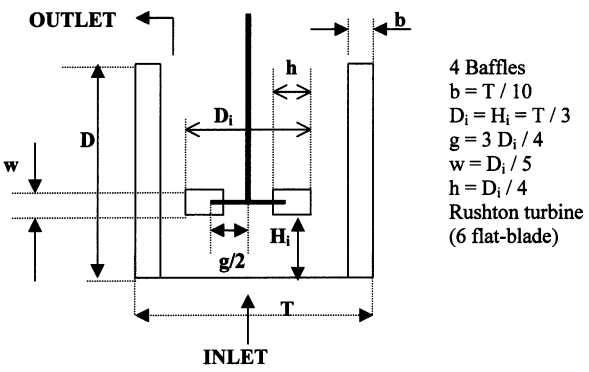

Fig. 1. Stirred tank characteristics.

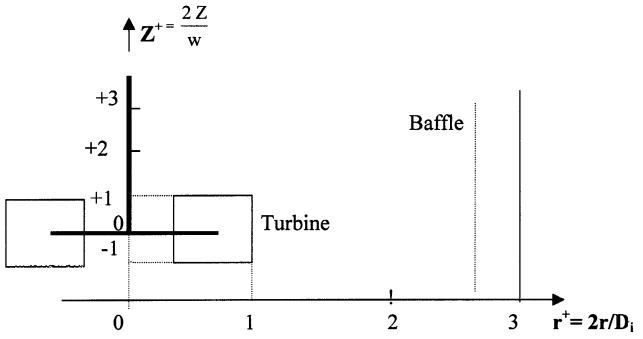

Fig. 2. Dimensionless coordinates used in the stirred tank reactor.

experiments were conducted in the conditions of an exponentially decreasing RTD with $\tau = V_{ol}/Q = 42\,s$.

4. Results

4.1. Third and fourth order statistical moments

We recall that these moments allow the comparison of the PDF of the fluctuations to Gaussian normal law characterizing the distribution of isotropic turbulence whose skewness ($S_k = \overline{k^3}/(\overline{k^2})^{3/2}$) and flatness ($F_k = \overline{k^4}/(\overline{k^2})^2$) factors, generally accepted values, are respectively 0 and 3 [31,32]. For further clarity, lines corresponding to these values are drawn on the figures dealing with the experimental determination of these moments.

The tangential velocity skewness factor S_{vo} seems to keep values fairly close to zero even when the plan of measurements changes from $Z^+ = +1$ to $Z^+ = +3$ (Figs. 3 and 4). The axial velocity skewness factor S_{vz} exhibits the same behavior except that near the wall it is negative for $Z^+ = +1$ and becomes positive for $Z^+ = +3$. Due to the reflection of the laser beams on the air-PMMA diopter, the measurements of the radial velocity component were limited to the zone

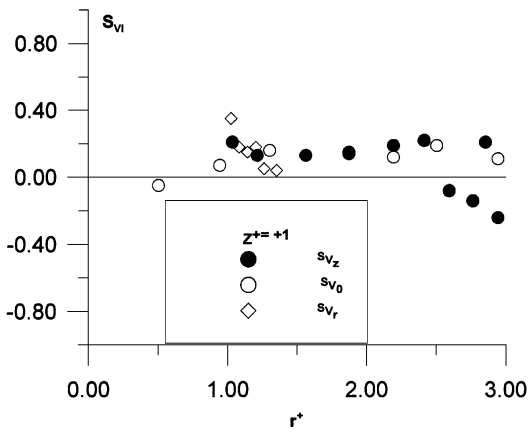

Fig. 3. Skewness factor relative to the three velocity components for the axial location $Z^+ = +1$.

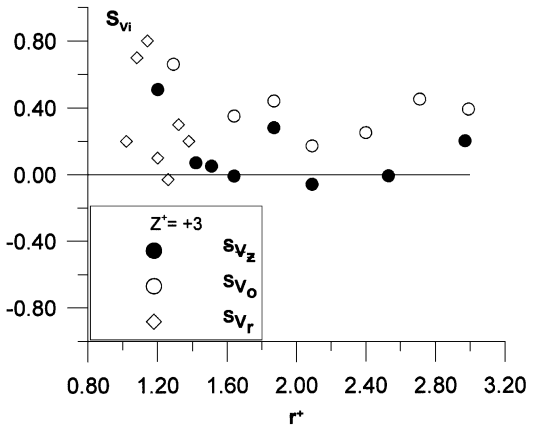

Fig. 4. Skewness factor relative to the three velocity components for the axial location $Z^+ = +3$.

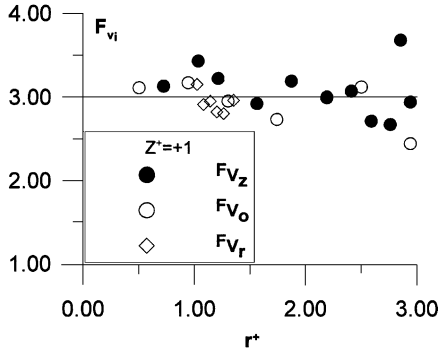

Fig. 6. Flatness factor relative to the three velocity components.

in the immediate proximity of the turbine ($r^+ = 2r/D_i < 1.40$). But in spite of this optical constraint and the scatter affecting the data, it may be mentioned that although positively skewed S_{vr} keeps values close to 0. For $Z^+ = 3$, the skewness factor for the three velocity components differs for $1.0 < r^+ < 1.3$. This can be explained by the interaction between the trailing vortex and the recirculation motion [22]. In view to appreciate the evolution of the skewness factor as function of the axial coordinate, S_{vz} versus the radius for $Z^+ = 0$, $Z^+ = \pm 1$, and $Z^+ = +3$ is drawn in Fig. 5. Although, due to baffles proximity S_{vz} deviates somewhat for $Z^+ = +1$, this parameter tends to remain around the value 0. Such tendency might indicate, at least, an axial homogeneity of the flow. Furthermore, the Gaussian distribution of S_{vz} in terms of the skewness factor is obvious indicating an absence of flow shearing and hence a tendency to local isotropy [31]. Stahl Wermesson and Tragarth [18] who conducted their experiments in a tank with slightly different conditions (two Rushton turbines, off-bottom clearance $H_i = 0.425D$ instead of $0.33D$) have found that S as well as F deviate notably from Gaussian values. The deviation of S and F from Gaussian values may found an explanation in the non-fully developed turbulence observed by these authors [18] when they measured the kinetic energy q and noted the drastic increase of this parameter with an increase of the agitation rate N.

For all the explored plans, the three velocity components flatness factors F_{vn} show values close to 3. Near the tank wall, the axial velocity flatness factor F_{vz} deviates a little from the Gaussian value (Fig. 6), as observed with S_{vz} hereabove. The behavior of the flatness factor F_{vz} is not significantly affected by a modification of the axial measurement plan coordinate as shown in Fig. 7. Indeed, to obtain an indication of the intermittency, if any, one can use the same procedure as Anandha and Brodkey [5] who define an intermittency factor by $\gamma = 3.0/F$. γ is close to 1 everywhere in the explored zone indicating the presence of a fully turbulent flow.

The concentration skewness factor S_{con} significantly deviates from the Gaussian value near the stirrer and particularly below (see Fig. 8; case $Z^+ = -1$). This behavior was

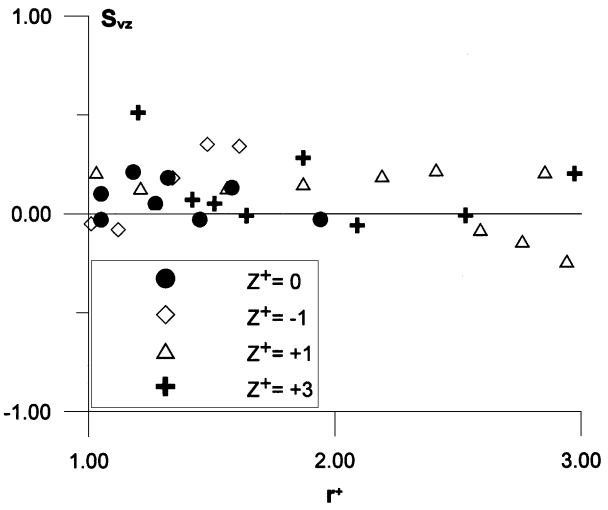

Fig. 5. Axial velocity skewness factor versus the tank radius.

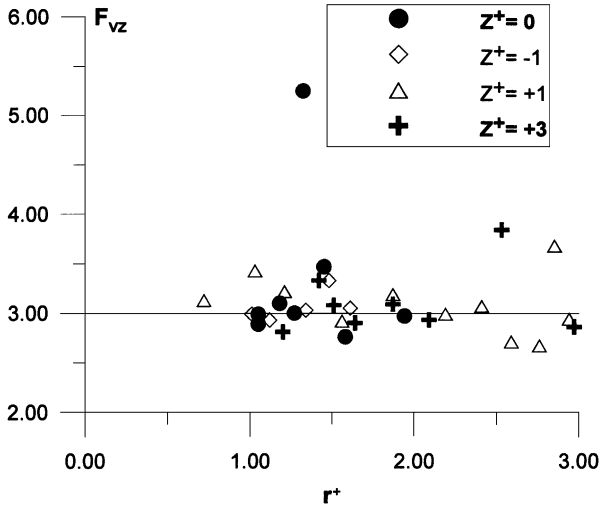

Fig. 7. Axial velocity flatness factor versus the tank radius.

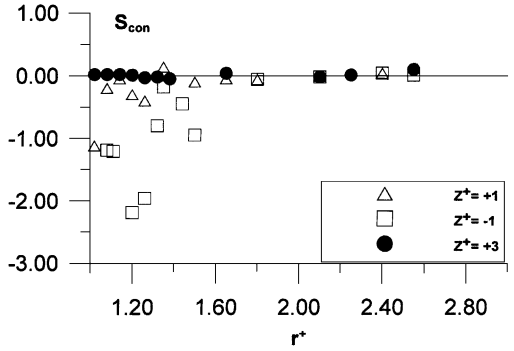

Fig. 8. Skewness factor relative to the concentration for different axial locations.

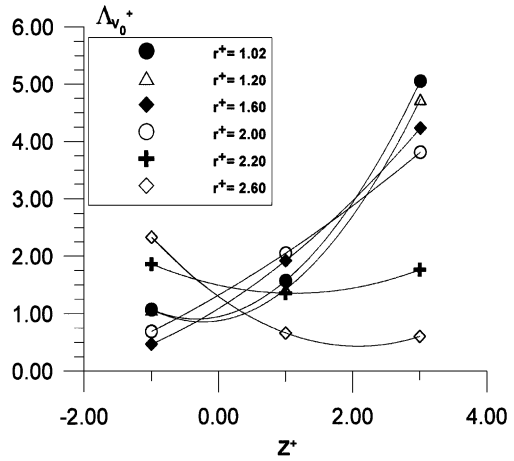

Fig. 9. Evolution of the tangential velocity integral scale versus the axial and radial locations.

expected since the tank is fed from the bottom and thus below the turbine the flow has no sufficient time to reduce the concentration gradients as observed also by Mahouast et al. [27] in almost the same conditions. The difference with respect to 0 is less marked just above the stirrer ($Z^+ = +1$) and disappears completely for a higher axial coordinate ($Z^+ = +3$), i.e. for a more efficient mixing. Far from the turbine ($r^+ > 1.50$), S_{con} is stabilised around 0.

Based on the results of skewness and flatness factors, it can be concluded that, in most cases, the probability density function of velocity as well as that of concentration fluctuations is almost Gaussian. The deviations observed in the vicinity of the stirrer and at the proximity of baffles are not to be considered because they are not significant. Hence, and as observed by Lee and Yianneskis [9], Nishikawa et al. [16] and Benayad et al. [21], turbulence may be assumed as locally isotropic far from the immediate proximity of the stirrer, in particular in the upper part of the tank with respect to the stirrer.

4.2. Reduced integral scales ($\Lambda_i{}^+ = \Lambda_i/w = 15\Lambda_i/D$)

When $Z^+ > 2$, the decrease in the dimensionless integral scale $\Lambda_{vo}{}^+$ relative to the tangential velocity as a function of r^+ is moderate for $1 < r^+ < 2$ and much faster for $r^+ > 2$ (Fig. 9). Furthermore, $\Lambda_{vo}{}^+$ generally increases rapidly with Z^+ except for $r^+ > 2.20$ where a decrease is first observed. Near the wall and thus near the baffles ($r^+ = 2.60$), $\Lambda_{vo}{}^+$ does not exceed 0.5 above the turbine ($Z^+ = 3$); however, this reduced scale can reach 5 near the stirrer and above the blades ($r^+ = 1.20$ and $Z^+ = 3$). It should be pointed out that our values are somewhat high compared to the literature (0.1–$1.0w < \Lambda_i < 0.3$–$3.0w$) [5,9,10,17,19,20]. This may be explained by the choice of the integral scale Λ_i studied which is the tangential one Λ_{vo}. Indeed, the zone where it exhibits high values is defined by $Z^+ = 3$ and $1.02 < r^+ < 2.00$. This area is not reached by the influence of the baffles which prevent the formation of the free vortex induced by the turbine rotation and hence reduce the eddies dimension. Being not limited in size in the tangential direction, the eddies will consequently have relatively larger integral scale $\Lambda_{vo}{}^+$. The dimensionless concentration integral scale $\Lambda_{con}{}^+$ increases as function of the radius r^+ when $Z^+ = \pm 1$ and r^+ is greater than 1.20 (Fig. 10). When $r^+ < 1.20$, the values of $\Lambda_{con}{}^+$ are practically identical for $Z^+ = \pm 1$. In the upper part of the tank and far from the turbine ($Z^+ = +3$), $\Lambda_{con}{}^+$ is almost constant at a lower value ($\Lambda_{con}{}^+ < 0.8$). This low value with respect to $\Lambda_{vo}{}^+$ shows that, in the upper part of the tank but far from the baffles, the concentration field structures are more dispersive compared to those of the velocity field.

4.3. Axial velocity–concentration correlation coefficient

The radial evolution of the correlation coefficient R_{cvz} is not regular (Fig. 11). Nevertheless, the values found are of the same order of magnitude as R_{cvr} and R_{cvo} coefficients [21]. In the immediate proximity of the turbine, these coefficients remain low (<5%). Their values in the plans $Z^+ = -1$ and $Z^+ = 0$ allow to calculate the turbulent diffusion

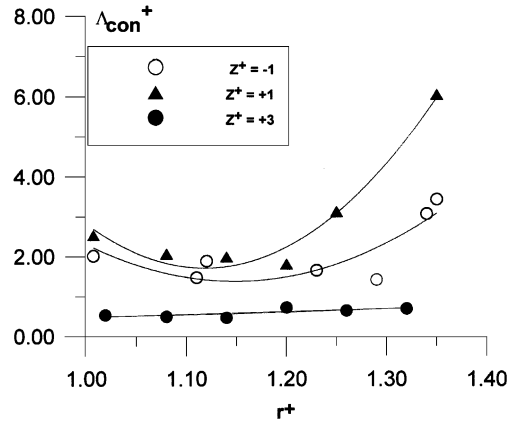

Fig. 10. Evolution of the concentration integral scale in function of the radius for different axial locations.

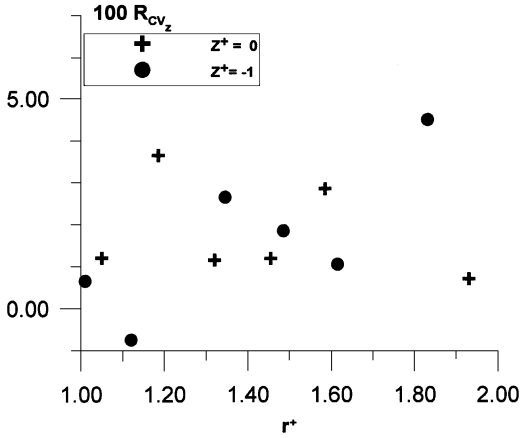

Fig. 11. Axial velocity–concentration correlation coefficient at the axial location $Z^+ = 0$ and $Z^+ = -1$.

coefficient. The spatial variation of D_t was small enough to consider D_t as constant at the value 7.4×10^{-2} cm^2/s. Taking into account the scattered data of Fig. 11, this value has to be considered as an acceptable approximation of the turbulent diffusion coefficient. The constant value of D_t means that the turbulent flux is proportional to the mean concentration gradient. Thus, with respect to the perfect macromixing and the local turbulence isotropy far from the stirrer, the micromixing may be considered as uniform in the tank. Although the value found is 3800 times greater than the KCl molecular diffusion coefficient D_m, it is 150 times lower than that reported by Nagata [15] in an agitated vessel. Nevertheless, our results seem rather acceptable than those reported by this author [15] which are, in our opinion, an over estimation of D_t due to the less accurate measurement method used. Indeed, Nagata [15] used a visualization based method and measured the extent of the plume generated by a dye injection.

5. Conclusion

The experimental study of velocity and concentration fields interaction in the three dimensional turbulent flow of a stirred tank reactor was achieved by coupling LDV and microconductimetry techniques. The results obtained are an additional contribution to the knowledge of the $\overline{c v_i}$ terms present in the governing equations of the turbulent mixing of an incompressible fluid with a passive scalar. An order of magnitude of turbulent diffusion coefficient D_t was also obtained (about $4000 D_m$). On the other hand, the hypothesis of isotropic turbulence was discussed and the probability density function of either velocities and concentration is found to not deviate significantly from Gaussian distribution indicating local isotropy conditions particularly far from the stirrer zone. Models using the results mentioned above and those concerned by mean values as well as Reynolds stresses reported elsewhere will allow to refine mixing models and numerical simulations.

References

[1] F.A. Holland, F.S. Chapman, Liquid Mixing and Processing in Stirred Tanks, Reinhold, New York, 1966.
[2] E.T. Sweeney, An Introduction and Literature Guide to Mixing, BHRA Fluid Engineering Series, British Library Cataloguing in Publication Data, Bedford, UK, Vol. 5, 1978.
[3] S. Benayad, Thèse de Doctorat de 3è Cycle, INPL Nancy, France, 1984.
[4] P. Siragna, Thèse de Doctorat d'Ingénieur, INPL Nancy, France, 1982.
[5] M. Anandha Rao, R.S. Brodkey, Chem. Eng. Sci. 27 (1972) 137.
[6] K. Van Der Molen, H.R.E. Van Maanen, Chem. Eng. Sci. 33 (1978) 1161.
[7] J.P. Barthole, J. Maisonneuve, J.N. Gence, R. David, J. Mathieu, J. Villermaux, Chem. Eng. Fund. 1 (1982) 17.
[8] S. Ito, K. Ogawa, N. Yoshida, J. Chem. Eng. Jpn. 8 (1975) 206.
[9] K.C. Lee, M. Yianneskis, AIChE J. 44 (1998) 13.
[10] H. Wu, G.K. Patterson, Chem. Eng. Sci. 44 (1989) 2207.
[11] H. Wu, G.K. Patterson, M. Van Dorm, Exp. Fluids 8 (1989) 153.
[12] M. Mahouast, Thèse de Doctorat de l'INPL, INPL Nancy, France, 1988.
[13] P. Mavros, I. Naude, C. Xuereb, J. Bertrand, Trans. IChemE, Part A 75 (1997).
[14] E. Stahl Wermesson, C. Tragarth, Chem. Eng. J. 72 (1999) 97.
[15] S. Nagata, Mixing Principles and Applications, Halsted Press, Wiley, New York, 1975.
[16] M. Nishikawa, Y. Okamoto, K. Hashimoto, S. Nagata, J. Chem. Eng. Jpn. 9 (1976) 489.
[17] J. Costes, J.P. Couderc, Chem. Eng. Sci. 43 (1988) 2765.
[18] E. Stahl Wermesson, C. Tragarth, Chem. Eng. J. 70 (1988) 37.
[19] M. Mahouast, G. Cognet, in: Proceedings of the Third International Symposium on Laser Anemometry, ASME, Boston, MA, December 13–18, 1987, pp. 127–134.
[20] S. Michelet, A. Kemoun, J. Mallet, M. Mahouast, Exp. Fluids 23 (1997) 418.
[21] S. Benayad, R. David, G. Cognet, Chem. Eng. Process. 19 (1985) 157.
[22] K. Rutherford, K.C. Lee, S.M.S. Mahmoudi, M. Yianneskis, AIChE J. 42 (1996) 332.
[23] F. Lemoine, M. Wolff, M. Lebouche, Exp. Fluids 20 (1996) 178.
[24] F. Lemoine, M. Wolff, M. Lebouche, CR Acad. Sci. Paris 325 Série II b (1997) 511.
[25] J.F. Brodberger, Thèse de Doctorat d'Ingénieur, INPL Nancy, France 1982.
[26] S. Gaskey, P. Vaccus, J.C. André, J. Villermaux, in: Proceedings of the Sixth European Conference on Mixing, Pavia, Italy, May 24–26, 1988.
[27] M. Mahouast, R. David, G. Cognet, Entropie 133 (1987) 7.
[28] S.Y. Ju, T.M. Mulvahill, R.W. Pike, Can. J. Chem. Eng. 68 (1990) 3.
[29] L.J. Chang, R.V. Mehta, J.M. Tarbell, Chem. Eng. Commun. 42 (1986) 139.
[30] Handbook of Chemistry and Physics, 55th Edition, Section F, CRC Press, Ohio, USA, 1974–1975, 60 pp.
[31] J.O. Hinze, Turbulence, McGraw-Hill, New York, 1975.
[32] J. Cousteix, Turbulence et Couche Limite, CEPADUES Edition, CEPAD, 1989, pp. 133–236.